

Neural Networks with Dynamic Synapses

Misha Tsodyks

Department of Neurobiology, Weizmann Institute of Science, Rehovot 76100, Israel

Klaus Pawelzik

Max-Planck-Institut für Strömungsforschung, D-37073 Goettingen, Germany

Henry Markram

Department of Neurobiology, Weizmann Institute of Science, Rehovot 76100, Israel

Transmission across neocortical synapses depends on the frequency of presynaptic activity (Thomson & Deuchars, 1994). Interpyramidal synapses in layer V exhibit fast depression of synaptic transmission, while other types of synapses exhibit facilitation of transmission. To study the role of dynamic synapses in network computation, we propose a unified phenomenological model that allows computation of the postsynaptic current generated by both types of synapses when driven by an arbitrary pattern of action potential (AP) activity in a presynaptic population. Using this formalism, we analyze different regimes of synaptic transmission and demonstrate that dynamic synapses transmit different aspects of the presynaptic activity depending on the average presynaptic frequency. The model also allows for derivation of mean-field equations, which govern the activity of large, interconnected networks. We show that the dynamics of synaptic transmission results in complex sets of regular and irregular regimes of network activity.

1 Introduction ---

A marked feature of synaptic transmission between neocortical neurons is a pronounced frequency dependence of synaptic responses to trains of presynaptic spikes (Thomson & Deuchars, 1994). The nature of this dynamic transmission varies among different classes of neurons. In our recent article (Tsodyks & Markram, 1996; see also Abbott, Varela, Sen, & Nelson, 1997; Tsodyks & Markram, 1997) we studied synaptic depression between neocortical pyramidal neurons with the aid of a phenomenological model. We found that the rate of depression is a primary factor in determining which features of the action potential (AP) activity in the presynaptic population are most effective in driving the postsynaptic neuron.

The phenomenological formulation of Tsodyks and Markram (1996) and Abbott et al. (1997) can be generalized to describe facilitating synapses be-

tween pyramidal cells and inhibitory interneurons (Thomson & Deuchars, 1994; Markram, Tsodyks, and Wang, in press). This formulation has two major goals. First, it allows the quantification of the features of the AP activity of the presynaptic neurons and populations transmitted by these different types of synapses. Second, it can be used in deriving a novel mean-field dynamics of neocortical networks aimed at understanding the dynamic behavior of large neuronal populations without having to solve an equally large number of equations. Mean-field descriptions were extensively used in order to understand the possible computations of cortical neural networks (see, e.g., Wilson & Cowan, 1972; Amit & Tsodyks, 1991; Ginsburg & Sompolinsky, 1994; Tsodyks, Skaggs, Sejnowski, & McNaughton, 1997). The novel formulation that uses the generalized phenomenological model of dynamic properties of synaptic connections between different types of neocortical neurons allows the study of the effects of synaptic dynamics and synaptic plasticity on information processing in large neural networks.

2 Phenomenological Model of Neocortical Synapses

In order to derive a coarse-grained description of neuronal dynamics, we have to compute the postsynaptic current generated by a population of neurons with a particular firing rate. This can be done with the phenomenological model of neocortical synapses used in Tsodyks and Markram (1997) and Abbott et al. (1997), which was shown to reproduce well the synaptic responses between pyramidal neurons. The model assumes that a synapse is characterized by a finite amount of resources. Each presynaptic spike (arriving at time t_{sp}) activates a fraction (U_{SE} , utilization of synaptic efficacy) of resources, which then quickly inactivate with a time constant of few milliseconds (τ_{in}) and recover with a time constant of about 1 second (τ_{rec}). The corresponding kinetic equations read:

$$\begin{aligned}\frac{dx}{dt} &= \frac{z}{\tau_{rec}} - U_{SE}x(t_{sp} - 0)\delta(t - t_{sp}) \\ \frac{dy}{dt} &= -\frac{y}{\tau_{in}} + U_{SE}x(t_{sp} - 0)\delta(t - t_{sp}) \\ \frac{dz}{dt} &= \frac{y}{\tau_{in}} - \frac{z}{\tau_{rec}},\end{aligned}\tag{2.1}$$

where x , y , and z are the fractions of resources in the recovered, active, and inactive states, respectively. The postsynaptic current is taken to be proportional to the fraction of resources in the active state, $I_s(t) = A_{SE}y(t)$. The two major parameters of the model are A_{SE} , the absolute synaptic strength, which can be exhibited only by activating all of the resources, and U_{SE} , which determines the dynamics of the synaptic response. For an individual synapse, the model reproduces the postsynaptic responses generated

by any presynaptic spike train t_{sp} for interpyramidal synapses in layer V (Tsodyks & Markram, 1997).

2.1 Modeling Facilitating Synapses. The formulation of equation 2.1 does not include a facilitating mechanism, which is not evident between pyramidal neurons. It is, however, prominent in synapses between pyramidal neurons and inhibitory interneurons (Thomson & Deuchars, 1994). A standard way of modeling short-term facilitation is by introducing a facilitation factor, which is elevated by each spike by a certain amount and decays between spikes, possibly at several rates (see, e.g., Mallart & Martin, 1967; Zengel & Magleby, 1982). To add facilitation into our synaptic model, we therefore assume that the value of U_{SE} is not fixed but is increased by a certain amount due to each presynaptic spike. The running value of U_{SE} is referred to as U_{SE}^1 . The resulting model includes both facilitating and depressing mechanisms.

Increase in U_{SE} could reflect, for example, the accumulation of calcium ions caused by spikes arriving in the presynaptic terminal, which is responsible for the release of neurotransmitter (Bertram, Sherman, & Stanely, 1996). For a simple kinetic scheme, assume that an AP causes a fraction of U_{SE} calcium channels to open, which subsequently close with a time constant of τ_{facil} . The fraction of opened calcium channels determines the current value of U_{SE}^1 . The corresponding kinetic equation therefore reads:

$$\frac{dU_{SE}^1}{dt} = -\frac{U_{SE}^1}{\tau_{facil}} + U_{SE}(1 - U_{SE}^1)\delta(t - t_{sp}). \quad (2.2)$$

U_{SE} determines the increase in the value of U_{SE}^1 due to each spike and coincides with the value of U_{SE}^1 reached upon the arrival of the first spike (in other words, at a very low frequency of stimulation).

This equation can be transformed into an iterative expression for the value of U_{SE}^1 reached upon the arrival of n th spike in a train, which determines the postsynaptic response according to equation 2.1,

$$U_{SE}^{1(n+1)} = U_{SE}^{1(n)}(1 - U_{SE})\exp(-\delta t/\tau_{facil}) + U_{SE}, \quad (2.3)$$

where δt is the time interval between the n th and $(n + 1)$ th spikes. If the presynaptic neuron emits a regular spike train at the frequency r , U_{SE}^1 reaches a steady value of

$$\frac{U_{SE}}{1 - (1 - U_{SE})\exp(-1/r\tau_{facil})}.$$

Thus in this formulation, U_{SE}^1 becomes a frequency-dependent variable, and U_{SE} is a kinetic parameter characterizing an activity-dependent transmission in a given synapse.¹

¹ One could introduce two independent parameters describing initial value and degree

Facilitating and depressing mechanisms are intricately interconnected since stronger facilitation leads to higher U_{SE}^1 values, which in turn leads to stronger depression. The value of U_{SE} therefore determines the contribution of facilitation in generating subsequent synaptic responses. Facilitation is marked for small values of U_{SE} and is not observed for higher U_{SE} . We found that the main features of synaptic transmission between pyramidal neurons and inhibitory interneurons are well captured by this model with $U_{SE} \sim 0.01 \rightarrow 0.05$, and τ_{rec} is typically several times faster than τ_{facil} (Markram et al., in press; see also Figure 1D). Figures 1A and 1B show responses from facilitating and depressing synapses with the same absolute strength to a regular spike train of 20 Hz (but with input resistance of the facilitatory synapse's target 10 times higher). Figure 1C illustrates the buildup of depression in facilitating synapses when they are stimulated at high frequencies. As a result, the stationary level of response exhibits a tuning curve dependence on the frequency, in agreement with experimental results (see Figure 1D).

3 Population Signal

We now return to our original problem of signaling from a large population of presynaptic neurons. There is an infinite number of ways the neurons of a population can fire relative to each other. Analysis of neurophysiological data revealed that individual neurons *in vivo* fire irregularly at all rates (Softky & Koch, 1993), reminiscent of the so-called Poisson process. Mathematically, the Poisson assumption means that at each moment, the probability that a neuron will fire is given by the value of the instantaneous firing rate and is independent of the timing of previous spikes. This assumption allows averaging equations 2.1 and 2.2 over different realizations of Poisson trains with a given rate, to obtain a new dynamics for the corresponding mean quantities (Amit & Tsodyks, 1991):

$$\begin{aligned}\frac{d\langle x \rangle}{dt} &= \frac{1 - \langle x \rangle}{\tau_{rec}} - \langle U_{SE}^1 \rangle \langle x \rangle r(t) \\ \frac{d\langle U_{SE}^- \rangle}{dt} &= -\frac{\langle U_{SE}^- \rangle}{\tau_{facil}} + U_{SE}(1 - \langle U_{SE}^- \rangle)r(t) \\ \langle U_{SE}^1 \rangle &= \langle U_{SE}^- \rangle(1 - U_{SE}) + U_{SE},\end{aligned}\tag{3.1}$$

where $r(t)$ denotes the rate of a Poisson train for the neuron at time t . $\langle U_{SE}^- \rangle$ denotes the average value of U_{SE}^1 immediately before the spike. Depressing synapses are described by the first of these equations with the fixed value of U_{SE}^1 (see also Grossberg, 1969, for the earlier analysis of these equations).

of facilitation of U_{SE}^1 . More data are required to determine whether this is needed to model facilitating synapses in neocortex accurately.

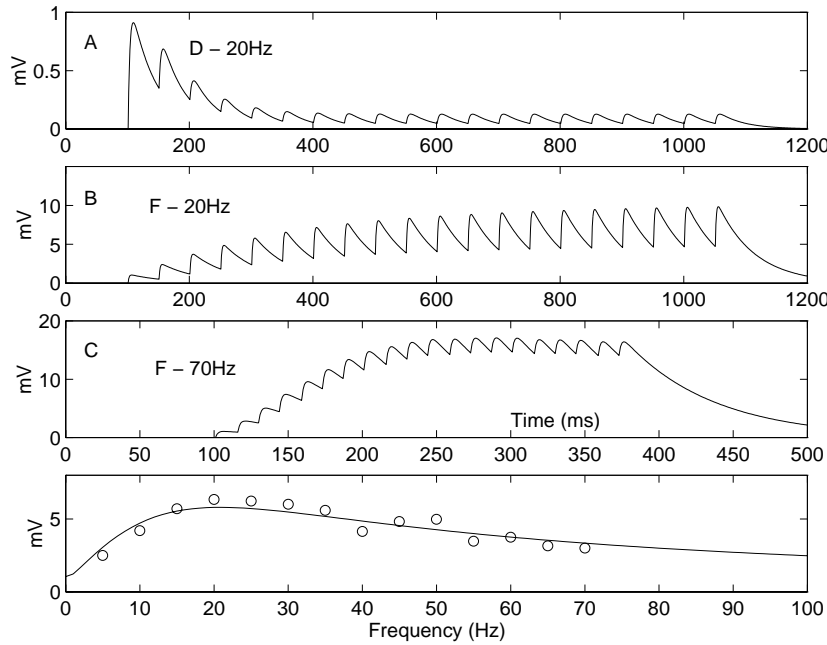


Figure 1: Phenomenological synaptic model. (A) Simulated postsynaptic potential generated by a regular spike train at a frequency of 20 Hz transmitted through a depressing synapse. (B) Same as A for facilitating synapse. (C) Same as B but for a presynaptic frequency of 70 Hz. (D) Stationary level of excitatory presynaptic potentials versus presynaptic frequency for facilitating synapses. Open circles: Experimental results for one of the recorded synaptic connections between pyramidal neuron and inhibitory interneuron (details of the experiments will be reported in Markram et al., in press). Solid line: Model results.

The postsynaptic potential is computed using a passive membrane mechanism ($\tau_{mem} \frac{dV}{dt} = -V + R_{in} I_{syn}(t)$) with an input resistance of $R_{in} = 100 \text{ M}\Omega$ for pyramidal target and $1 \text{ Giga}\Omega$ for interneuron. Parameters: (A): $\tau_{mem} = 40 \text{ msec}$; $\tau_{inact} = 3 \text{ msec}$; $A_{SE} = 250 \text{ pA}$; $\tau_{rec} = 800 \text{ msec}$; $U_{SE} = 0.5$; (BCD) $\tau_{mem} = 60 \text{ msec}$; $\tau_{inact} = 1.5 \text{ msec}$; $A_{SE} = 1540 \text{ pA}$; $\tau_{rec} = 130 \text{ msec}$; $\tau_{facil} = 530 \text{ msec}$; $U_{SE} = 0.03$;

In deriving equation 3.1, we made a further simplification by assuming that the inactivation time constant τ_{in} is much faster than the recovery one τ_{rec} . This assumption is valid for interpyramidal synapses studied in Markram and Tsodyks (1996) and for pyramidal interneuron synapses (Markram et al., in press). The evolution of postsynaptic current can be obtained from

the remaining equation for y and recalling that $I_s(t) = A_{SE}y(t)$:

$$\frac{d\langle y \rangle}{dt} = -\frac{\langle y \rangle}{\tau_{in}} + \langle U_{SE}^1 \rangle \langle x \rangle r(t), \quad (3.2)$$

which can be simplified to $y = r\tau_{in}U_{SE}^1\langle x \rangle$ if one is interested only in the timescale slower than τ_{in} .

While averaging equation 2.1 over different realizations of Poisson spike trains, we assumed that there is no statistical dependence between the variables $x(t)$ and $U_{SE}^1(t)$ and the probability of spike emission at time t . This is strictly valid only if there is no facilitation since in this case U_{SE}^1 is a fixed parameter of the model, and $x(t)$, which is a function of the spike arrival times prior to the current time, is independent of the probability of a spike at time t due to the Poisson assumption. However, if facilitation is included, both $x(t)$ and $U_{SE}^1(t)$ are a function of previous spikes and are not statistically independent. We thus performed simulations of equations 2.1 and 2.2 for populations of presynaptic neurons firing Poisson spike trains with various modulations of their firing rate and compared the resulting postsynaptic current with the solution of the mean-field equation 3.1. We found that in all cases considered, mean-field solutions were good approximations (see, e.g., Figure 2). More detailed analysis, outlined in the appendix, showed that mean-field approximation works because for all frequencies, either U_{SE}^1 or x have small coefficients of variation (CV), and thus the effect of the statistical correlations between them is small.

Equations 3.1 and 3.2 can be solved analytically for an arbitrary modulation of the firing rates of the presynaptic population. In the case of depressing synapses, the solution takes a particular simple form:

$$\langle y(t) \rangle = U_{SE}r(t) \int_{-\infty}^t dt' \exp\left(-\frac{t-t'}{\tau_{rec}} - \int_{t'}^t dt'' U_{SE}r(t'')\right). \quad (3.3)$$

We use this equation to determine which features of the presynaptic AP train are transmitted by depressing synapses to their targets. Assuming that the presynaptic frequency changes gradually, one can write down the expansion over the derivatives of the frequency. The first two terms of this expansion are,

$$\frac{r}{1+rU_{SE}\tau_{rec}} + r' \frac{r}{(1+rU_{SE}\tau_{rec})^3} + \dots \quad (3.4)$$

This expression describes the relative contribution of rate and temporal signaling in generating the postsynaptic response. The first term depends on the current rate, which is dominant for frequencies that are small compared to the limiting frequency $\lambda \sim 1/(U_{SE}\tau_{rec})$. As the frequency increases, this term saturates, and thus progressively less rate signaling is possible.

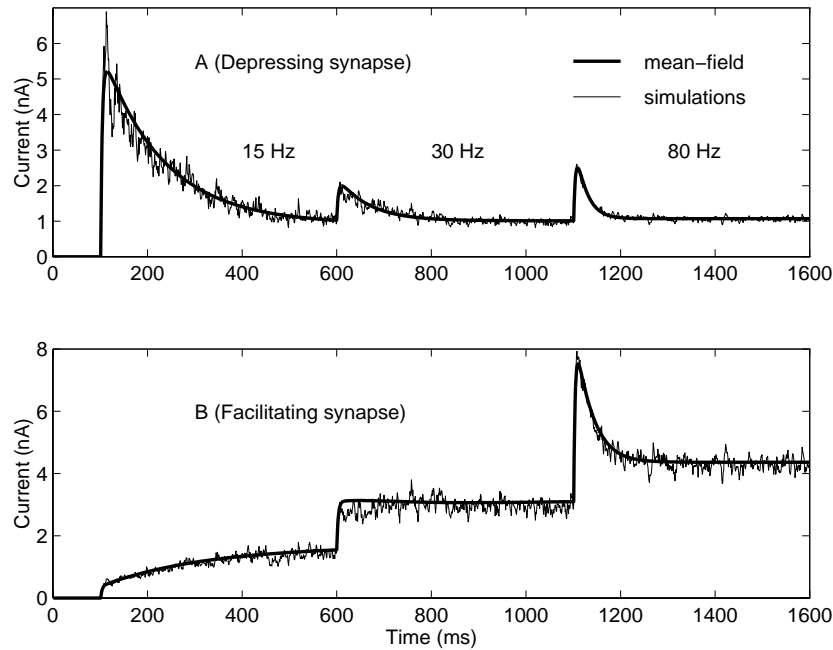


Figure 2: Postsynaptic current, generated by Poisson spike trains of a population of 1000 neurons with synchronous transitions from 0 Hz to 15 Hz to 30 Hz and then to 80 Hz, transmitted through facilitating (A) and depressing (B) synapses. Thick line: Solution of mean-field equation 3.1 and 3.2. Thin line: Simulations of 1000 spike trains with the use of the full model in equation 2.1. Parameters are the same as in Figure 1, with $A_{SE} = 250$ pA.

The main contribution at higher frequencies therefore comes from a transient term reflecting the changes in frequencies. In the context of population signaling, this means that only synchronous transitions in the population activity can be signaled to the postsynaptic neuron (Tsodyks & Markram, 1997).

The solution of the full set of equations 3.1 for facilitating synapse has the same form as equation 3.4, with the single complication due to the fact that U_{SE}^1 is now a functional of the frequency

$$U_{SE}^1 = U_{SE} \int_{-\infty}^t dt' r(t') \exp \left(-\frac{t-t'}{\tau_{facil}} - U_{SE} \int_{t'}^t dt'' r(t'') \right), \quad (3.5)$$

which has to be substituted in equation 3.3. One could still analyze the qualitative features of this solution by noting that at very high frequencies, $U_{SE}^1 \rightarrow 1$, and thus facilitating synapses behave in the same way as depressing ones, transmitting the information about the rate transitions. As the frequency decreases toward the peak frequency (see Figure 1D),

$$\theta = 1/\tau_{facil} + \sqrt{2/\tau_{facil}^2 + \frac{1 + U_{SE}}{U_{SE}\tau_{rec}\tau_{facil}}} \approx 1/\sqrt{U_{SE}\tau_{rec}\tau_{facil}}, \quad (3.6)$$

the presynaptic rate dominates in the postsynaptic response. The reason is that at this frequency, facilitating and depressing effects compensate each other, and the average amplitude of excitatory postsynaptic potential (EPSP), which is $\sim xU_{SE}^1$, is approximately constant. At even smaller frequencies, depressing effects become less relevant since x recovers almost to unity between the subsequent spikes. In this regime, the postsynaptic signal mainly reflects the current value of rate amplified by the value of U_{SE}^1 :

$$I_s \sim r(t) \int_{-\infty}^t dt' r(t') \exp(-(t-t')/\tau_{facil}). \quad (3.7)$$

The integral in this equation is roughly equal to the number of spikes emitted by the presynaptic neuron in the preceding time window of τ_{facil} . In this regime, postsynaptic response is a delayed and amplified transformation of the presynaptic frequency.

As an example, we show in Figure 2 the postsynaptic current resulting from a series of transitions in the firing rate for both depressing and facilitating synapses. All three regimes of transmission via facilitating synapses are illustrated in Figure 2B.

4 Mean-Field Network Dynamics

The analysis of the previous section allows the formulation of a closed system of equations for the dynamics of a large network consisting of subpopulations of neurons with uniform connections. Each population could describe a cortical column, which consists of neurons with similar receptive field properties. At this stage, we assume that at each cortical location, there are only two subpopulations of cortical neurons: pyramidal excitatory neurons and inhibitory interneurons. The coarse-grained equations, describing the firing rates of these populations, have the same form as in Wilson and Cowan (1972) and Amit and Tsodyks (1991),

$$\tau_e \frac{dE_r}{dt} = -E_r + g \left(\sum_{r'} J_{rr'}^{ee} y_{r'}^{ee} - J_{rr'}^{ei} y_{r'}^{ei} + I_r^e \right)$$

$$\tau_i \frac{dI_r}{dt} = -I_r + g \left(\sum_{r'} J_{rr'}^{ie} y_{r'}^{ie} - J_{rr'}^{ii} y_{r'}^{ii} + I_r^i \right), \quad (4.1)$$

where $E_r(I_r)$ is the firing rate of excitatory (inhibitory) populations located at the site r ; $g(x)$ is a response function usually assumed to be monotonously increasing; and $J_{rr'}^{ee}$ denotes the absolute strength of the synaptic connection between excitatory neurons in the populations located at r and r' times the average number of such connections per one postsynaptic neuron, correspondingly for other interactions. Finally, I_r^e (I_r^i) is the external input to the excitatory (inhibitory) population. $y_{rr'}^{ee}$ (and corresponding values for all other synapses) has to be computed from equations 3.1 and 3.2 for each connection rr' with the corresponding set of kinetic parameters. Refractoriness of the neurons was ignored for simplicity.

These equations reduce to the ones of Wilson and Cowan (1972) if synaptic transmission is frequency independent, in which case $x_r \equiv 1$ and hence $y_r \sim E_r$. In the presence of frequency dependence, they include effects of ever-changing synaptic efficacy due to depression and facilitation. This formulation allows for an analysis of the behavior of the network with any pattern of connections and external inputs. Since the goal of this article is not to consider any particular computational model, we limit ourselves to two examples.

4.1 Network of One Population. As the simplest example, we consider a network that consists of only one population of excitatory neurons. Already in this case, synaptic depression makes the network dynamics nontrivial. Equations 4.1 reduce to,

$$\begin{aligned} \tau \frac{dE}{dt} &= -E(t) + g(JU_{SE}x(t)E(t)) \\ \frac{dx}{dt} &= -U_{SE}E(t)x(t) + \frac{1-x(t)}{\tau_{rec}}. \end{aligned} \quad (4.2)$$

For convenience, the factor of τ_{in} (see equation 3.2) was absorbed in the definition of J . We can solve these equations for the fixed point, where it simplifies to,

$$E = g \left(JU_{SE} \frac{E}{1 + EU_{SE}\tau_{rec}} \right) \quad (4.3)$$

and can be illustrated using the graphical method (see Figure 3A). The right-hand side of equation 4.3 always saturates for arbitrary response functions due to synaptic depression. The system will therefore have a nontrivial fixed point with $E > 0$, even in cases where without depression there is no stable solution.

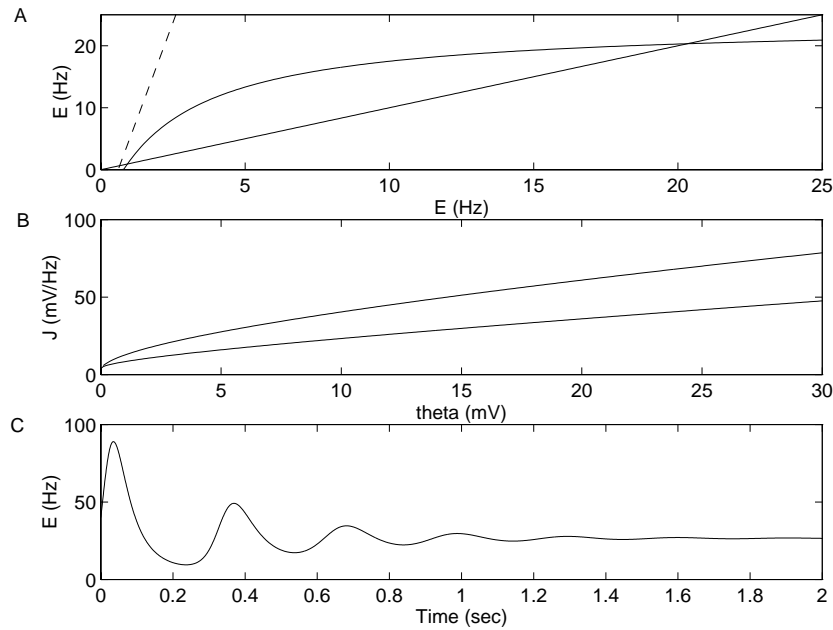


Figure 3: Solution of equations 4.2 for the network of one excitatory population with homogeneous connections. (A) Graphical solution of the fixed-point equation, 4.3. The response function had a linear-threshold shape (dashed line),

$$g(x) = \begin{cases} 0 & \text{if } x < \theta \\ \beta(x - \theta) & \text{if } x > \theta \end{cases} \quad (4.4)$$

The fixed-point solution is given by the intersection of the two solid lines. (B) Phase diagram of the system in the space of θ and J . (C) The solution of the dynamic equations, 4.2.

Parameters in (A) and (C): $\theta = 15$ mV; $\beta = 0.5$ mV⁻¹Hz; $J = 60$ mV*Hz⁻¹; $U_{SE} = 0.5$; $\tau_{rec} = 800$ msec; $\tau = 30$ msec.

The stability of the fixed-point solution can be analyzed from equations 4.2. The solution is stable if the following matrix has eigenvalues with negative real parts:

$$\begin{pmatrix} \frac{\beta J U_{SE} x^* - 1}{\tau} & \frac{\beta J U_{SE} E^*}{\tau} \\ -U_{SE} x^* & -U_{SE} E^* - \frac{1}{\tau_{rec}} \end{pmatrix}, \quad (4.5)$$

where E^* and x^* are the values of E and x at the fixed point, $\beta = g'(J U_{SE} x^* E^*)$. For a linear-threshold gain function ($\beta = \text{const}$) as in Figure 3A, the phase

diagram of the system is shown in Figure 3B. For a given threshold, a fixed-point solution appears when the synaptic strength exceeds the first critical value shown by the lower line on the diagram. Contrary to what one would expect from Figure 3A, this solution remains unstable until the synaptic strength grows above a second critical value (upper line).

Even if the fixed-point solution is stable, the system exhibits dampened oscillations before reaching the steady state due to synaptic dynamics (see Figure 3C).

4.2 Network of Two Interconnected Populations. This system was analyzed in Wilson and Cowan (1972) for the case of linear synapses. They showed that if the external inputs are fixed, mean-field equations have two basic types of stable solutions: fixed points and limit cycles with the period on the order of τ_e, τ_i . In our case, the mean-field equations have a much richer set of solutions, because in addition to the pair of equations for E and I (see equation 4.1), they also include dynamic equations for synaptic efficacies (see equation 3.1). As a result, in addition to fixed points and simple limit cycles, the system exhibits a variety of rhythmic and irregular solutions that dominate the network behavior but are difficult to analyze in a completely general manner. Two particular novel solutions, one periodic and another irregular, are shown in Figures 4A and 4B.

5 Conclusion

In this study, we introduce a phenomenological model that allows computation of the postsynaptic responses generated by either facilitating or depressing synapses for an arbitrary train of presynaptic spikes. The model was used to define the signals that can be transmitted by these synapses, and we show that signaling through these two types of synapses is fundamentally different at low firing rates but becomes more similar as the firing rate grows.

The model was also used to test the validity of the derivation of self-consistent mean-field equations for the dynamic behavior of large neural networks with arbitrary architecture of external inputs and internal interactions. The formalism was illustrated by considering two simple examples of networks consisting of one and two uniform populations of neurons. The purely excitatory network was shown always to possess a fixed-point solution, which can have arbitrary small firing rates. Adding an inhibitory population greatly increases the repertoire of behaviors, including the irregular sequence of population bursts of various amplitudes. Synaptic dynamics could therefore be an important factor in generating different states of cortical activity as reflected by electroencephalogram recordings.

An important challenge for the proposed formulation remains in analyzing the influence of the synaptic dynamics on the performance of other,

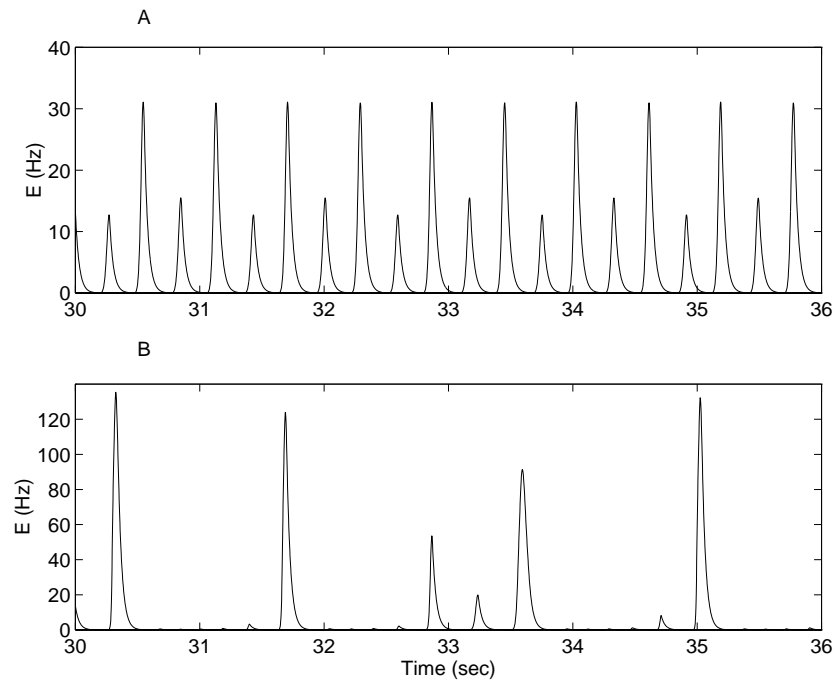


Figure 4: Solutions of equation 4.1 for the network of two populations with homogeneous connections. (A) Population activity $E(t)$ for the parameters $I^e = 17$ mV; $I^i = 15$ mV; $J_{ee} = 50$ mV*Hz $^{-1}$; $J_{ei} = 40$; $J_{ie} = 70$; $J_{ii} = 19.5$; $U_{SE} = 0.5$ (ee and ei); $U_{SE} = 0.05$ (ie); 0.03 (ii); $\tau_{rec} = 800$ msec (ee and ei); 600 msec (ie); 850 msec (ii); $\tau_{facil} = 1000$ msec (ie); 400 msec (ii); $\tau_e = 30$ msec; $\tau_i = 40$ msec. (B) The same as in A but with $J_{ii} = 0$. The gain functions for both populations have the same form as in Figure 3.

computationally more instructive neural network models. Work in this direction is in progress.

Note added in proof: After the work was completed, we learned that a network of excitatory population can have oscillating solutions under some conditions (J. Rinzel, private communication).

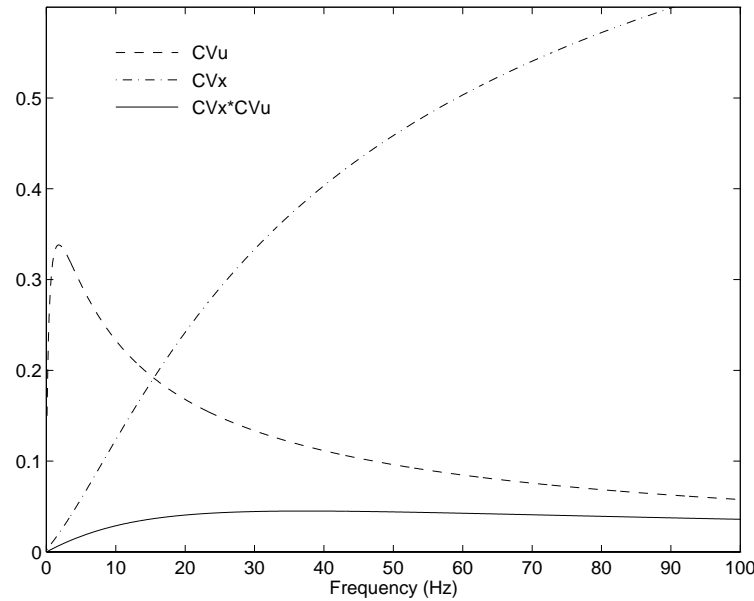


Figure 5: Coefficients of variation of U_{SE} , x , as well as their product, as a function of presynaptic frequency. Parameters are the same as in Figures 1B–D.

Appendix

The mean-field description in section 3 was derived by adopting an approximation,

$$\langle x U_{SE}^1 \rangle = \langle x \rangle \langle U_{SE}^1 \rangle. \quad (\text{A.1})$$

The relative error of this approximation can be estimated using the Cauchy-Schwarz inequality of the probability theory:

$$\frac{|\langle x U^1 \rangle - \langle x \rangle \langle U^1 \rangle|}{\langle x \rangle \langle U^1 \rangle} \leq CV_x CV_U, \quad (\text{A.2})$$

where CV_x (CV_U) stay for the coefficient of variation of the random variable x (U^1); we use U^1 instead of U_{SE}^1 for brevity. Intuitively, this inequality states that if one of the random variables has a small CV, its correlations with the other variables can be neglected. We can now use equation 2.2 to compute the CV of U_{SE}^1 for any presynaptic rate r . In the steady state, the result of

computation is,

$$CV_U^2 = \frac{r\tau_{facil}(1-U)^2}{2(1+r\tau_{facil})^2(1+Ur\tau_{facil}(1-U/2))}. \quad (\text{A.3})$$

CV_x can be computed from equation 2.1, again assuming the condition in equation A.1:

$$CV_x^2 = \frac{r\tau_{rec}\langle(U^1)2/2\rangle}{1+r\tau_{rec}\langle U^1(1-U1/2)\rangle}. \quad (\text{A.4})$$

The self-consistency of the mean-field theory can now be checked by plotting the product of CV_U and CV_x as a function of frequency (see Figure 5). The graph shows that for the set of parameters used in modeling facilitating synapses, derived from experimental traces, the relative error of equation A.1 does not exceed 5 percent for any frequency. More detailed analysis of equations A.3 and A.4 indicates that this error can exceed a 10 percent level only at the significantly shorter τ_{facil} and higher values of U at which the model does not exhibit facilitating behavior anymore.

Acknowledgments

This study was supported by grants from the Office of Naval Research and the Minerva Foundation. We thank Andreas Herz for discussions and two referees for useful comments on the article.

References

- Abbott, L. F., Varela, J. A., Sen, K., & Nelson, S. B. (1997). Synaptic depression and cortical gain control. *Science*, 275, 220–224.
- Amit, D. J. & Tsodyks, M. V. (1991). Quantitative study of attractor neural network retrieving at low spike rates I: Substrate-spikes, rates, and neuronal gain. *Science*, 2, 259–274.
- Bertram, R., Sherman, A., & Stanely, E. F. (1996). Single-domain/bound calcium hypothesis of transmitter release and facilitation. *J. Neurophysiol.*, 75, 1919–1931.
- Ginsburg, I., & Sompolinsky, H. (1994). Theory of correlations in stochastic neural networks. *Phys. Rev. E*, 50, 3171–3191.
- Grossberg, S. (1969). On the production and release of chemical transmitters and related topics in cellular control. *J. Theor. Biol.*, 22, 325–364.
- Mallart, A., & Martin, A. R. (1966). Two components of facilitation at the neuromuscular junction of the frog. *J. Physiol.*, 193, 677–694.
- Markram, H., & Tsodyks, M. V. (1996). Redistribution of synaptic efficacy between pyramidal neurons. *Nature*, 382, 807–810.
- Markram, H., Tsodyks, M., & Wang, Y. (In press). Differential signaling via the same axon of neocortical pyramidal neurons. *Proc. Nat'l Acad. Sci. USA*.

- Softky, W. R., & Koch, C. (1993). The highly irregular firing of cortical cells is inconsistent with temporal integration of random EPSPs. *J. Neurosci.*, *13*, 334–350.
- Thomson, A. M., & Deuchars, J. (1994). Temporal and spatial properties of local circuits in neocortex. *Trends in Neurosci.*, *17*, 119–126.
- Tsodyks, M. V., & Markram, H. (1996). Plasticity of neocortical synapses enables transitions between rate and temporal coding. *Lect. Notes Comput. Sci.*, *1112*, 445–450.
- Tsodyks, M. V., & Markram, H. (1997). The neural code between neocortical pyramidal neurons depends on neurotransmitter release probability. *Proc. Nat'l Acad. Sci. USA*, *94*, 719–723.
- Tsodyks, M. V., Skaggs, W. E., Sejnowski, T., & McNaughton, B. L. (1997). Paradoxical effect of external modulation of inhibitory neurons. *J. Neurosci.*, *17*, 4382–4388.
- Wilson, H. R., & Cowan, J. D. (1972). Excitatory and inhibitory interneurons. *Biophys.*, *12*, 1–24.
- Zengel, J. E., & Magleby, K. L. (1982). Augmentation and facilitation of transmitter release: A quantitative description at the frog neuromuscular junction. *J. Gen. Physiol.*, *80*, 583–611.

Received February 26, 1997; accepted October 30, 1997.